NBS1 binds directly to TOPBP1 via disparate interactions between the NBS1 BRCT1 domain and the TOPBP1 BRCT1 and BRCT2 domains

Oanh Huynh[1], Kenna Ruis[1], Katrina Montales[1], and W. Matthew Michael[1,2]

[1]Molecular and Computational Biology Section

Department of Biological Sciences

University of Southern California

Los Angeles, CA 90089

[2]Author for correspondence at: mattm@usc.edu

Abstract

The TOPBP1 and NBS1 proteins are key components of DNA repair and DNA-based signaling systems. TOPBP1 is a multi-BRCT domain containing protein that plays important roles in checkpoint signaling, DNA replication, and DNA repair. Likewise, NBS1, which is a component of the MRE11-RAD50-NBS1 (MRN) complex, functions in both checkpoint signaling and DNA repair. NBS1 also contains BRCT domains, and previous works have shown that TOPBP1 and NBS1 interact with one another. In this work we examine the interaction between TOPBP1 and NBS1 in detail. We report that NBS1 uses its BRCT1 domain to interact with TOPBP1's BRCT1 domain and, separately, with TOPBP1's BRCT2 domain. Thus, NBS1 can make two distinct contacts with TOPBP1. We report that recombinant TOPBP1 and NBS1 proteins bind one another in a purified system, showing that the interaction is direct and does not require post-translational modifications. Surprisingly, we also report that intact BRCT domains are not required for these interactions, as truncated versions of the domains are sufficient to confer binding. For TOPBP1, we find that small 24-29 amino acid sequences within BRCT1 or BRCT2 allow binding to NBS1, in a transferrable manner. These data expand our knowledge of how the crucial DNA damage response proteins TOPBP1 and NBS1 interact with one another and set the stage for functional analysis of the two disparate binding sites for NBS1 on TOPBP1.

Key words

BRCT domain, TOPBP1, NBS1, MRN complex, protein-protein interaction, scaffold protein

36 **1. Introduction**

37 The BRCA1 C-terminal (BRCT) domain is an interaction module that allows
38 the host protein to bind to various biological substrates such as other proteins,
39 nucleic acids, and poly (ADP-ribose) chains (reviewed by Gerloff et al, 2012; Leung
40 and Glover, 2011; Reinhardt and Yaffe, 2013; Wan et al, 2016). BRCT proteins are
41 major players in the DNA damage response (DDR), and it is therefore crucial that we
42 understand how they function and that we fully describe all the different modes by
43 which they interact with their binding partners. Regarding how BRCT domains bind
44 to other proteins, there are two general categories: interactions that require the
45 BRCT binding substrate to be phosphorylated, and those that do not. For phospho-
46 driven interactions, some BRCT domains contain a so-called phosphate-binding
47 pocket (PBP), which features a triad of conserved amino acid residues that interact
48 with the phosphate group on the substrate protein (reviewed by Leung and Glover,
49 2011; Reinhardt and Yaffe, 2013; Wan et al, 2016; Day et al, 2021). BRCT domains
50 that bind phospho-epitopes are typically found in pairs, where one domain within
51 the pair contains the PBP. While the PBP directly interacts with phosphate, both
52 BRCT domains within the pair are required for binding as the PBP forms via
53 intramolecular interactions between the two domains (reviewed by Leung and
54 Glover, 2011; Reinhardt and Yaffee, 2013; Day et al, 2021). Intramolecular
55 interactions between BRCT domains also allow binding of the host protein to
56 substrate in a phospho-independent manner, and both the phospho-dependent and
57 independent modes of binding have been observed within the same protein. The
58 yeast Rtt107 protein contains 6 BRCT domains, with the C-terminal two BRCTs

59 supplying phospho-dependent binding to histone H2A, and the four N-terminal
60 domains forming a compact, higher-order assembly that binds peptide ligands from
61 a number of proteins (Wan et al, 2019). The net result is that Rtt107 binds to
62 chromatin via the phospho-dependent mechanism, and then recruits other proteins
63 to chromatin via the phospho-independent mechanism.
64
65 BRCT domains also make intermolecular contacts to allow assembly of both
66 homo- and heterotypic multimers. A well-studied example of BRCT::BRCT
67 intermolecular interaction is found with the XRCC1 and DNA Ligase 3 (LIG3)
68 proteins (Taylor et al, 1998; Dulic et al, 2001; Beernink et al, 2005; Cuneo et al,
69 2011; London, 2015; London et al, 2020; Hammel et al, 2021) . Both proteins can
70 homodimerize via BRCT::BRCT interaction, and the two can also heterodimerize via
71 their BRCT domains. Recent work from our group was focused on the
72 Topoisomerase II Binding Protein 1 (TOPBP1) protein, which contains nine BRCT
73 domains, and we found that TOPBP1 forms oligomers and that the protein is capable
74 of a series of BRCT::BRCT interactions (Kim et al, 2020). More specifically, we found
75 that BRCT1&2 could bind to BRCT domains 1,2, and 5, and that BRCT4&5 could bind
76 BRCTs 1 and 2 but not 5. In this work we examine how TOPBP1 uses its BRCT
77 domains to bind a heterologous protein, by studying its interaction with the NBS1
78 protein.
79
80 NBS1 is part of a trimeric complex, termed MRN for MRE11-RAD50-NBS1,
81 that senses DNA double-strand breaks (DSBs) and then plays multiple roles in

82 ensuring efficient repair of the breaks (reviewed by McCarthy-Leo et al, 2022;
83 Reginato and Cejka, 2020; Syed and Tainer, 2018). These roles include holding the
84 two broken ends together, initiating DNA end resection, and activation of the DNA
85 damage checkpoint kinases ATM and ATR. MRN activates ATM directly (reviewed by
86 Paull, 2015), and ATR indirectly through its ability to recruit TOPBP1 to the DSB
87 (Montales et al, 2022). Recent work from our laboratory has shown that loss of MRN
88 attenuates ATR signaling at DSBs, and TOPBP1's occupancy at the DSB is also
89 reduced (Montales et al, 2022). TOPBP1 has a well-studied function in directly
90 interacting with ATR (and its binding partner ATRIP) at sites of damage to stimulate
91 ATR kinase activity (reviewed by Wardlaw et al, 2015), and thus our recent work
92 has revealed a pathway for ATR signaling that runs from the DNA end through MRN
93 to TOPBP1 and then ATR (Montales et al, 2022). One open and important question
94 for this pathway is: what is the molecular mechanism by which MRN recruits
95 TOPBP1 to DSBs?
96
97 In this study we focused on the NBS1 subunit as previous works have shown
98 that TOPBP1 and NBS1 bind one another, and that this interaction is conserved from
99 frogs to man (Morishima et al, 2007; Yoo et al, 2009). Interestingly, in both frogs and
100 humans, TOPBP1 and NBS1 constitutively bind to one another, and the interaction is
101 then enhanced during the DSB response (Morishima et al, 2007; Yoo et al, 2009).
102 Here, we study the constitutive interaction, and we find that NBS1 uses its BRCT1
103 domain to make direct contacts with TOPBP1's BRCT1 domain and, separately, the
104 BRCT2 domain. Our data provide a molecular explanation for how MRN recruits

105 TOPBP1 to DSBs, and they also expand our understanding of how BRCT::BRCT

106 interactions drive the cellular response to DNA damage.

107

108 **2. Material and Methods**

109 *2.1 Materials*

110 *2.1.1 Plasmids*

111 The expression vector to produce GST-RAD9 Tail has previously been
112 described (Duursma et al., 2013). All other plasmids used in this study are
113 described below, in table format, and all are *Xenopus* proteins. Specific details about
114 plasmid construction are available upon request.

115

Plasmid	Name	Vector	AA coordinates
5Xmyc-BRCT0-2	pHG128	pCS2+MT	1-333
5Xmyc-BRCT0-2 KK155,249EE	pAK42	pCS2+MT	1-333
5Xmyc-BRCT4&5	pJA19	pCS2+MT	480-758
5Xmyc-BRCT0	pHG126	pCS2+MT	1-99
5Xmyc-BRCT1	pHG129	pCS2+MT	100-191
5Xmyc-BRCT2	pJA23	pCS2+MT	191-333
5Xmyc-NBS1	pKM107	pCS2+MT	1-763
5Xmyc-NBS1 1-400	pKM105	pCS2+MT	1-400
5Xmyc-NBS1 1-200	pKR34	pCS2+MT	1-200
5Xmyc-NBS1 1-100	pOH4	pCS2+MT	1-100
5Xmyc-NBS1 100-200	pKR36	pCS2+MT	100-200
5Xmyc-NBS1 200-400	pKR37	pCS2+MT	200-400
5Xmyc-NBS1 393-763	pKM106	pCS2+MT	393-763
5Xmyc-NBS1 1-400 K158A	pOH34	pCS2+MT	1-400
5Xmyc-NBS1 1-175	pOH35	pCS2+MT	1-175

5Xmyc-NBS1 1-150	pOH36	pCS2+MT	1-150
5Xmyc-NBS1 128-400	pOH39	pCS2+MT	128-400
5Xmyc-NBS1 128-400	pOH40	pCS2+MT	150-400
MBP-TOPBP1 1-333	pAK53	pUC57-MBP	1-333
MBP-TOPBP1 91-275	pAK56	pUC57-MBP	91-275
MBP-TOPBP1 91-196	pKR23	pUC57-MBP	91-196
MBP-TOPBP1 91-179	pKR24	pUC57-MBP	91-179
MBP-TOPBP1 91-156	pKR25	pUC57-MBP	91-156
MBP-TOPBP1 91-139	pKR26	pUC57-MBP	91-139
MBP-TOPBP1 128-179	pKR29	pUC57-MBP	128-179
MBP-TOPBP1 138-179	pKR30	pUC57-MBP	138-179
MBP-TOPBP1 128-156	pKR38	pUC57-MBP	128-156
MBP	pOH10	pUC57-MBP	-
MBP-TOPBP1 221-273	pOH6	pUC57-MBP	221-273
MBP-TOPBP1 231-273	pOH7	pUC57-MBP	231-273
MBP-TOPBP1 221-250	pOH8	pUC57-MBP	221-250
MBP-TOPBP1 197-231	pOH9	pUC57-MBP	197-231
MBP-TOPBP1 242-273	pOH11	pUC57-MBP	421-273
MBP-TOPBP1 250-273	pOH12	pUC57-MBP	250-273

2.1.2 Recombinant proteins

The recombinant proteins used in this study were GST, GST-NBS1 1-400, GST-NBS1 1-400 K158E, GST-NBS1 393-763, GST-RAD9Tail, GST-BRCT4&5, MBP, MBP-BRCT1&2, and 6His-T7-BRCT0-2. Expression vectors for GST-RAD9Tail (Duursma et al., 2013), GST-BRCT4&5, MBP-BRCT1&2, and 6His-T7-BRCT0-2 (Kim

122 et al, 2020) have been described. Expression vectors for GST-NBS1 1-400, GST-NBS1
123 1-400 K158E, and GST-NBS1 393-763 were made using pGEX4T-3 as the backbone.
124 All proteins were expressed in *E. coli* BL21(DE3) cells, at 37°C for 4 hours, and all
125 proteins were purified from the soluble fraction according to standard procedures
126 (detailed below).
127
128 *2.1.3 Antibodies*
129 We used the following commercially sourced antibodies in this work: Myc
130 (Millipore Sigma #M4439), MBP (New England Biolabs #E8032S), GST (Millipore
131 Sigma #05-782), and T7 (Millipore Sigma #69522). We also used our own antibody
132 against *Xenopus* TOPBP1, HU142, which has been described (Van Hatten et al.,
133 2002).
134
135 *2.2 Methods*
136 *2.2.1 Xenopus egg extracts (XEE)*
137 Extracts were prepared as previously described (Van Hatten et al., 2002, Yan
138 et al., 2006).
139
140 *2.2.2 IVTT production of proteins and determination of protein concentrations*
141 In-vitro transcription and translation (IVTT) reactions were performed using
142 the SP6 TnT® Quick Coupled Transcription/Translation System (Promega #L2080)
143 according to the manufacturer's instructions. For Bug-Bunny binding assays we
144 used 20µl of the IVTT reaction/sample.

145

146 *2.2.3 Recombinant Protein Expression and Purification*

147 Plasmids were transformed in BL21 (DE3) Competent *E. Coli* cells and grown
148 in LB media (GST fusion proteins) or LB media with 0.2% glucose (MBP fusion
149 proteins) with ampicillin. At an OD600 of 0.6-0.8, cells were induced with 0.3 mM
150 IPTG for 4 hours at 37˚C. Cells were then harvested by centrifugation (4000 rpm for
151 20 min) and washed with phosphate-buffered saline (PBS). Cells were lysed by
152 sonication in GST column buffer (40% PBS, 60% TEN buffer: 10 mM Tris-Cl, pH 8.0,
153 1 mM EDTA, pH 8.0, 100 mM NaCl) supplemented with complete protease inhibitor
154 cocktail tablets (Roche #04693159001) and 10 mg lysozyme for GST fusion proteins
155 or in maltose column buffer (20 mM Tris-HCl, pH 7.4, 0.3 M NaCl, and 1 mM EDTA)
156 with 1mM DTT and complete protease inhibitor cocktail tablets for MBP fusion
157 proteins. Lysates were cleared by centrifugation (15,000 rcf for 20 min) and
158 incubated with glutathione sepharose (BioVision #6566) for GST fusion proteins or
159 amylose resin (New England Biolabs #E8021S) for MBP fusion proteins for 1 hour at
160 4˚C. Beads were poured over a column and washed with column buffer. GST fusion
161 proteins were eluted with 20 mM glutathione in 75 mM HEPES, pH 7.5, 150 mM
162 NaCl, 5 mM DTT, and 0.1% Triton-X. MBP fusion proteins were eluted with 10 mM
163 maltose in maltose column buffer. Proteins were dialyzed overnight into PBS.

164

165 *2.2.4 Protein binding assays*

166 Three kinds of protein binding assays were utilized. The first involved the
167 addition of recombinant proteins to XEE (Figures 1B-D). For these assays 25 µl of

168 XEE was supplemented with 5 µg of GST-tagged recombinant protein. DSBs, in the
169 form of EcoRI-digested lambda DNA, were also optionally added (500 ng). After a
170 30-minute incubation the samples were diluted into 400 µl of Binding Buffer (PBS +
171 0.1% NP-40) and incubated with glutathione sepharose (BioVision, #6566). The
172 beads were washed four times with 500 µl of Binding Buffer and then eluted with 2X
173 Sample Buffer (Millipore Sigma #S3401-10VL). The total and bound fractions were
174 then analyzed via Western blotting using standard conditions. The second involved
175 incubation of IVTT proteins with recombinant GST or MBP fusion proteins purified
176 from *E. coli,* in what we refer to as the Bugs-Bunny system. For these assays 20 µl of
177 IVTT proteins were mixed with 5 µg of GST or MBP fusion protein and incubated for
178 60 minutes at 30°C. The mixtures were diluted into 400 µl of Binding Buffer and
179 then incubated with the appropriate resin (amylose for MBP, New England Biolabs
180 # E8021S; glutathione sepharose for GST, BioVision #6566) for one hour at 4°C.
181 The beads were washed four times with 500 µl of Binding Buffer and then eluted
182 with 2X Sample Buffer. The input and bound fractions were then analyzed via
183 Western blotting using standard conditions. The third type of binding assay (done
184 once, in Figure 4F) was a variant of the pull-down where MBP recombinant proteins,
185 purified from *E. coli,* were mixed at 10 µg each with 100 ng of 6His-T7-BRCT0-2, also
186 purified from *E. coli.* The samples were then treated as described above for the
187 Bugs-Bunny system. ImageJ software was used to quantify the signal intensity of
188 bound and input samples, and the percent of bound to input was presented in
189 Figure 2C.
190

191 **3. Results**

192 *3.1 The TOPBP1-NBS1 interaction can be recapitulated using E. coli- and IVTT-*
193 *produced proteins.*

194 Previous work from many different laboratories has shown that TOPBP1 and
195 MRN act together to promote DDR signaling, and that NBS1 and TOPBP1 can bind to
196 one another, although how this interaction occurs is not known (Morishima et al,
197 2007; Yoo et al, 2009; Duursma et al., 2013; Shiotani et al, 2013; Montales et al,
198 2022). The domain structures of the two proteins are shown in Figure 1A. As
199 detailed above, TOPBP1 contains nine BRCT domains, named 0-8. NBS1 is less
200 complex, with three protein-protein interaction motifs, two BRCT domains and one
201 FHA domain. One previous study analyzed the interaction between TOPBP1 and
202 NBS1 in some detail (Yoo et al, 2009). Using *Xenous* egg extracts, Yoo and colleagues
203 found that TOPBP1 and NBS1 could co-precipitate under resting conditions, and
204 that the interaction was enhanced when DDR signaling was activated. This work
205 went on to show that TOPBP1 uses its BRCT0-2 region to bind NBS1, and that the
206 relevant region within NBS1 mapped to the amino-terminal 400 amino acids of the
207 protein. We have recently shown that MRN is important for recruitment of TOPBP1
208 in frog egg extracts to long, linearized dsDNA templates that mimic DSBs (Montales
209 et al, 2022). Given these findings, we were motivated to analyze the TOPBP1-NBS1
210 interaction in more detail.

211

212 We first sought to repeat some of the earlier findings by Yoo and colleagues
213 (Yoo et al, 2009), that a fragment of *Xenopus* NBS1 corresponding to amino acids 1-

214 400 could bind to *Xenopus* TOPBP1 after incubation in frog egg extracts.
215 Accordingly, we expressed and purified from *E. coli* a GST-NBS1 1-400 fusion
216 protein. This protein, along with GST alone, was added to egg extract in either the
217 presence or absence of linearized 5kb dsDNA, which we have previously shown will
218 potently activate both ATR and ATM in our extracts (Montales et al, 2021; Ruis et al,
219 2022; Montales et al, 2022). The GST protein complexes were then recovered back
220 out of the extract, using glutathione-sepharose beads, and the presence of
221 endogenous TOPBP1 was detected via Western blotting. As displayed in Figure 1B,
222 TOPBP1 did not bind to GST alone, but it did bind to GST-NBS1 1-400. Binding was
223 evident in the sample lacking DSBs and was modestly enhanced by the presence of
224 DSBs. We next asked if there are additional binding sites for TOPBP1 within NBS1,
225 beyond those present in the 1-400 region, and we found that this is not likely as
226 TOPBP1 did not bind to a GST fusion containing NBS1 from residue 393 to the end
227 of the protein, amino acid 763 (Figure 1C). Lastly, we wanted to confirm that the
228 BRCT0-2 region of TOPBP1 could bind to NBS1 1-400, and for this a myc-tagged
229 TOPBP1 fragment corresponding to BRCT0-2 was produced by *in vitro* transcription
230 and translation (IVTT) and added to egg extract along with GST-NBS1 1-400. DSBs
231 were optionally added, and we observed that myc-TOPBP1 BRCT0-2 could readily
232 bind to GST-NBS1 1-400, but not to GST alone, and that binding was modestly
233 enhanced by DSBs (Figure 1D). Taken together, the data in Figures 1A-D are all in
234 excellent agreement with the previous work (Yoo et al, 2009).
235

236 As shown here, and by others, a constitutive interaction between TOPBP1
237 and NBS1 occurs in egg extract even in the absence of DDR signaling (Figures 1B-D;
238 Yoo et al, 2009). We wanted to study this basal interaction further, and we first
239 asked if we could recapitulate it using a protein-binding assay that we nicknamed
240 Bugs-Bunny (Figure 2A). In the Bugs-Bunny system one binding partner is
241 expressed and purified from *E. coli* (Bugs) and the other is synthesized by IVTT in
242 rabbit reticulocyte lysates (Bunny). After synthesis of one binding partner by IVTT
243 we simply add the purified form of the other partner to the rabbit reticulocyte
244 lysates. After incubation the samples are diluted in binding buffer and protein
245 complexes isolated using an affinity resin corresponding to the tag on the *E. coli*
246 produced protein (for this study the tag is predominantly GST, but sometimes MBP).
247 This system has several advantages for the study of protein-protein interactions.
248 One, the endogenous proteins present in the reticulocyte lysates help to prevent
249 non-specific binding of the target protein to the resin. Two, as detailed below, the
250 reticulocyte lysates can contain modifying enzymes, such as casein kinase 2 (CK2),
251 that are important for certain interactions. Three, and most importantly, because
252 synthesis of a target protein by IVTT is far less labor intensive than purification of
253 the target from bacterial or insect cells, one can rapidly screen through a collection
254 of mutants to analyze sequence determinants required for the interaction. Lastly, in
255 our experience, proteins are much better behaved, in terms of proper folding and
256 solubility, when made by IVTT relative to other expression systems.
257

258 We first examined binding of GST-NBS1 1-400 to myc-tagged TOPBP1
259 BRCT0-2 in the Bugs-Bunny assay. These are both derivatives of the *Xenopus*
260 proteins, as are all the factors analyzed in this study. As shown in Figure 2B, myc-
261 BRCT0-2 could bind to GST-NBS1 1-400 under these assay conditions, but not to
262 GST alone. These data show that the NBS1::TOPBP1 interaction is readily observed
263 using the Bugs-Bunny system, and thus that egg extract is not required for the
264 interaction to occur. We next assessed the specificity of the interaction between
265 NBS1 and TOPBP1's BRCT0-2 region by asking if NBS1 could also bind to TOPBP1's
266 BRCT4&5 domains. Binding assays were run with the following partners: GST-NBS1
267 1-400 with myc-tagged TOPBP1 BRCT0-2 or 4&5 domains, and GST fused to the
268 RAD9 Tail domain (RAD9Tail) with the same pair of TOPBP1 proteins. We included
269 RAD9Tail because we had previously shown that it binds well to myc-BRCT0-2 in
270 our Bugs-Bunny system (Kim et al, 2020). As shown in Figure 2C, myc-BRCT0-2
271 could bind both NBS1 and the RAD9Tail, and myc-BRCT4&5 failed to bind efficiently
272 to either NBS1 or RAD9Tail. Quantification revealed that binding of myc-TOPBP1
273 BRCT0-2 to NBS1 was slightly more efficient than binding to RAD9Tail, and that
274 binding of myc-BRCT4&5 to either GST substrate was largely undetectable. We
275 conclude that the Bugs-Bunny system faithfully recapitulates a specific interaction
276 between NBS1 and TOPBP1.
277
278 Both BRCT1 and BRCT2 from TOPBP1, as well as BRCT1 from NBS1, contain
279 PBPs, suggesting that the TOPBP1::NBS1 interaction may be phospho-dependent.
280 Previous work from our group has shown that the interaction between TOPBP1 and

281 the RAD9Tail, which requires phosphorylation of RAD9Tail, can be recapitulated in
282 the Bugs-Bunny system and this is because the reticulocyte lysates used for IVTT
283 contain CK2, the kinase responsible for RAD9Tail phosphorylation (Kim et al, 2020).
284 Thus, we next asked if including phosphatase in the binding assay would prevent
285 the NBS1::TOPBP1 interaction, as it does the RAD9Tail::TOPBP1 interaction. Myc-
286 BRCT0-2 was produced by IVTT and, prior to addition of the GST fusion proteins,
287 the samples were optionally treated with lambda phosphatase. As expected,
288 phosphatase treatment eliminated the RAD9Tail::TOPBP1 interaction, however the
289 NBS1::TOPBP1 interaction was refractory to phosphatase treatment (Figure 2D).
290 We conclude that the NBS1::TOPBP1 interaction does not require the presence of
291 phosphate on either binding partner.
292
293 *3.2 NBS1 can bind to both BRCT1 and BRCT2 of TOPBP1*
294 To pursue these observations, we next asked if NBS1 required an intact
295 BRCT0-2 region to associate with TOPBP1. To explore this, we subdivided TOPBP1's
296 BRCT0-2 region into the individual BRCT domains and tested them for binding to
297 NBS1. Surprisingly, both BRCT1 and BRCT2 could bind to NBS1 (Figure 3A),
298 whereas BRCT0 could not. In addition, while NBS1 readily binds the isolated BRCT1
299 or BRCT2 domains, the same is not true of RAD9Tail, as it could only interact with
300 the contiguous BRCT0-2 region, and not the individual BRCT1 or BRCT2 domains
301 (Figure 3B). Taken together, the data presented in Figures 1-3 show that the
302 TOPBP1 BRCT0-2 region interacts with NBS1 in a fundamentally different manner
303 than it does with RAD9Tail. The RAD9Tail::TOPBP1 interaction requires an intact

304 BRCT0-2 region and is dependent on phosphorylation (summarized in Figure 3C),
305 whereas the NBS1::TOPBP1 interaction requires neither an intact BRCT0-2 region
306 nor phosphorylation (Figure 3D).
307
308 *3.3 NBS1 uses its BRCT1 domain to bind TOPBP1.*
309 We next examined the sequence determinants within NBS1 that allow
310 binding to TOPBP1's BRCT1&2 region. The constructs used for this are summarized
311 in Figure 4A. We first confirmed that full-length NBS1 could bind TOPBP1's
312 BRCT1&2 domains in the Bugs-Bunny system, and to do so we employed an MBP-
313 TOPBP1 BRCT1&2 fusion protein purified from *E. coli*, together with myc-tagged
314 NBS1, made by IVTT. As shown in Figure 4B, full-length myc-NBS1 can bind MBP-
315 TOPBP1 BRCT1&2, but not MBP alone. We also observed that MBP- TOPBP1
316 BRCT1&2 could bind the NBS1 1-400 region, but not the 393-763 region (Figure
317 4C). These data show that despite switching production of the TOPBP1 region from
318 IVTT to *E. coli*, and vise-versa for NBS1, the ability to interact was not altered. We
319 next used MBP-TOPBP1 BRCT1&2 to delineate the region within NBS1 to which it
320 binds. The N-terminal portion of NBS1 was subdivided into three fragments, 1-100
321 (FHA domain), 100-200 (BRCT1), and 200-400 (BRCT2 plus additional sequences,
322 see Figure 4A), and we observed that only the BRCT1 domain could bind to TOPBP1
323 BRCT1&2 (Figure 4D). Thus, unlike TOPBP1 where both BRCT1 and BRCT2 bind
324 NBS1, for NBS1 just BRCT1 and not BRCT2 binds to TOPBP1.
325

326 *3.4 Direct interaction between NBS1 and TOPBP1.*

327 An important question became is the NBS1::TOPBP1 interaction direct, or
328 does it require a bridging factor that might be present in the reticulocyte lysates
329 used for our binding assays? To answer this we expressed and purified an MBP-
330 NBS1 1-200 fusion protein from *E. coli* (Figure 5A). We attempted to purify MBP-
331 NBS1 100-200, however we found that this protein was insoluble and difficult to
332 express in *E. coli*. We also produced a 6His-T7-TOPBP1 BRCT0-2 recombinant
333 protein (Figure 5A), one that we have used in the past (Kim et al, 2020). Thus, in this
334 experiment, both proteins were expressed in *E. coli* and then purified, thereby
335 eliminating concerns about bridging factors. To block non-specific binding to the
336 resin the assays were performed in binding buffer supplemented with 1% BSA. As
337 shown in Figure 5B, 6His-T7-TOBP1 BRCT0-2 could readily bind MBP-NBS1 1-200,
338 but not MBP alone, and binding was not inhibited by inclusion of phosphatase. We
339 conclude that the interaction between NBS1 and TOPBP1 is direct and does not
340 require any post-translational modifications on either partner.

341

342 *3.5 No requirement for phosphate-binding pockets in the TOPBP1::NBS1 interaction.*

343 Our recent study (Kim et al, 2020), together with data shown here, have
344 demonstrated that TOPBP1's BRCT1&2 region interacts with several different BRCT
345 domains, including TOPBP1's BRCT1, BRCT2, and BRCT5 domains as well as BRCT1
346 from NBS1 (Figure 5C). One feature that all these domains have in common is a PBP.
347 Even though we have shown that phosphate *per se* is not needed for the
348 TOPBP1::NBS1 interaction (Figures 2D and 5B), it was still possible that the PBPs

349 played a role in the binding. To test this idea we produced mutant proteins where a
350 key and highly conserved lysine residue within the PBP was mutated. For TOPBP1
351 we mutated both K155 in BRCT1 and K249 in BRCT2 to glutamic acid, in the context
352 of a myc-tagged BRCT0-2 fragment. Previous work with human TOPBP1 has shown
353 that a similar K to E substitution in BRCT1 prevents binding to RAD9 (Rappas et al,
354 2011), however we observed that the KK155,249EE double mutant could still
355 readily bind to GST-NBS1 1-400 (Figure 5D). For NBS1, we initially made the same K
356 to E mutation at K158 in BRCT1 and observed that this mutant could not bind to
357 TOPBP1 (data not shown). Because this charge-reversal mutation might non-
358 specifically disrupt folding of the NBS1 domains we also tested a more subtle
359 mutation, substituting K158 with alanine. The K158A mutation is still expected to
360 inactivate the PBP, as has been shown for the BRCA1 PBP (Botuyan et al, 2004),
361 however we observed that it had no impact on binding to TOPBP1 (Figure 5E). Thus,
362 for both TOPBP1 and NBS1, an intact PBP is dispensable for their interaction.
363
364 *3.6 Intact BRCT domains are not required for the TOPBP1::NBS1 interaction.*
365 To learn more about the NBS1::TOPBP1 interaction we asked how creating
366 truncations of TOPBP1's BRCT0-2 region would impact binding to NBS1 1-400. A
367 series of deletion mutants were constructed as fusions to MBP and are shown in
368 Figure S2A. These MBP fusions were produced by IVTT and tested for binding
369 against GST-tagged NBS1 1-400. We found that MBP-BRCT0-2 (amino acids 1-333)
370 and MBP-BRCT1&2 (amino acids 91-275) could bind NBS1 (Figure S2B). We next
371 asked if the linker sequence between BRCTs 1 and 2 influenced binding of BRCT1,

372 by comparing a construct containing the linker (amino acids 91-196) to one that
373 does not (amino acids 91-179). As shown in Figure S2B, both proteins could bind
374 NBS1. Moving forward, we next asked if BRCT1 must be in an intact form to bind to
375 NBS1. Structural analysis of BRCT domains has shown that they are highly ordered,
376 using a series of alpha helices and beta sheets to fold into a unit with a conserved
377 topology (reviewed by Gerloff et al, 2012; Leung and Glover, 2013; Reinhardt and
378 Yaffe, 2013; Wan et al, 2016). Thus, our expectation was that by making deletions
379 within BRCT1 the domain would lose its ability to fold properly and binding to NBS1
380 would be lost. This, however, was not the case. The Conserved Domain sequence
381 analysis tool that is available on the NCBI Structure website
382 (www.ncbi.nlm.nih.gov/Structure/cdd/wrpsb.cgi) defines *Xenopus* TOPBP1 BRCT1
383 as running from amino acid 108 to 179. As shown in Figure 6A&B, and we observed
384 that a fragment containing amino acids 128-179, and therefore missing the N-
385 terminal 20 amino acids of BRCT1, could bind well to NBS1. A slightly smaller piece,
386 corresponding to amino acids 138-179, could not bind NBS1 (Figure 6B). Intrigued
387 by these observations we next asked if loss of C-terminal sequences within
388 TOPBP1's BRCT1 would impact binding to NBS1. We found that truncation of the C-
389 terminal 23 amino acids of BRCT1, using a construct containing amino acids 91-156,
390 did not disrupt binding and, furthermore, that an even smaller fragment, amino
391 acids 128-156, could bind efficiently to NBS 1 1-400 (Figure 6C). Thus, an intact
392 BRCT1 domain is not required for its interaction with NBS1. To see if this is also true
393 of TOPBP1's BRCT2 we generated a series of deletion constructs (Figure S2C) and
394 tested them for binding to GST-NBS1 1-400. These results showed that a small

395 fragment of 23 amino acids, corresponding to residues 250-273, was sufficient for
396 binding to NBS1 (Figures S2D&E). We conclude that small sequences within both
397 BRCT1 and BRCT2 of TOPBP1 can confer binding to NBS1 onto a heterologous
398 protein, in this case MBP.
399
400 We next examined sequence determinants within the NBS1 BRCT domain
401 that allow binding to TOPBP1. For this we generated the series of deletion mutants
402 shown in Figure 6D, and we tested them for binding to *E. coli*-produced MBP-
403 TOPBP1 BRCT1&2. As expected, we found that the fragment corresponding to intact
404 FHA and BRCT1 domains (1-200) could bind efficiently to TOPBP1 (Figure 6E). We
405 also observed that a fragment where the carboxyl terminal 25 amino acids of BRCT1
406 were removed (1-175) retained the ability to bind TOPBP1. Thus, like TOPBP1's
407 BRCT1&2 domains, NBS1's BRCT1 domain can be truncated without attenuating the
408 interaction. We then asked if removing more of the carboxyl terminal sequences
409 impacted binding and found that neither a fragment corresponding to amino acids
410 1-150 nor one corresponding to 1-128 could bind TOPBP1. We also examined
411 amino-terminal deletions and found that removing the amino-terminal half of the
412 NBS1 BRCT1 domain did little to inhibit the interaction with TOPBP1 (Figure 6E).
413 These data show that, like TOPBP1's BRCT1 and BRCT2 domains, the NBS1 BRCT1
414 domain need not be in an intact and properly folded configuration to bind TOPBP1.
415
416 Data presented thus far show that, for all the relevant BRCT domains in this
417 study, binding persists even after truncation of the domain. These curious results

418 inspired us to ask if the interaction required that at least one partner contain an
419 intact BRCT domain. For example, if the NBS1 BRCT1 domain and the TOPBP1
420 BRCT1 domain are both in a truncated form, would the interaction be lost? As it
421 turned out, the answer is no. For this experiment we used an assay system where
422 both binding partners were produced by IVTT. This was because all the required
423 constructs for this experiment were available for protein production by IVTT, and
424 thus there was no need to remake them for expression in *E. coli*. Proteins were
425 produced by IVTT and then the lysates were mixed, to allow interaction. The
426 samples were then diluted in binding buffer and incubated with maltose beads,
427 followed by washing, elution, and Western blotting. As shown in Figure 6F, binding
428 was readily observed when the BRCT1 domains for both TOPBP1 and NBS1 were
429 intact (lane 1). Similarly, binding was observed when TOPBP1 BRCT1 was intact and
430 NBS1 BRCT1 was truncated (lane 2), and vise versa (lane 3). These results are all in
431 accordance with the data derived from the Bugs-Bunny assays shown in Figures 6B,
432 C, and E. When both binding partners where in a truncated form we also observed
433 efficient binding (lane 4), and binding was not observed when the NBS1 derivative
434 was truncated further (lane 5), consistent with data shown in Figure 6E. Based on
435 these data, we conclude that neither the TOPBP1 BRCT1 domain nor its counterpart
436 in NBS1 need to be in an intact and properly folded configuration for the interaction
437 to occur.
438

439 **4. Discussion**

440 In this study we examined how two crucial DDR proteins, TOPBP1 and NBS1,
441 interact with one another. Prior to this work, it was known that TOPBP1 and NBS1
442 can form a complex, in a manner conserved from frogs to man (Morishima et al,
443 2007; Yoo et al, 2009). However, it was not known which domains within either
444 protein control the interaction, and neither was it known if the interaction was
445 direct or mediated by a bridging factor. Here, we show that the NBS1 BRCT1 domain
446 binds both the BRCT1 and BRCT2 domain from TOPBP1. These are specific
447 interactions, as revealed by our finding that NBS1 binds well to TOPBP1 BRCTs 1&2
448 but shows very little affinity for BRCTs 4&5 (Figure 2C). Likewise, TOPBP1 binds
449 NBS1 BRCT1 efficiently but there is no detectable binding to either the FHA or
450 BRCT2 domains from NBS1 (Figure 4D). Our data also show that the interaction
451 between TOPBP1 and NBS1 is constitutive, and it is also direct and independent of
452 any post translational modifications (Figure 5). Thus, at least a subset of MRN
453 complexes contain TOPBP1 even under resting conditions. In our previous work we
454 showed that immunodepletion of MRN from frog egg extracts with antibodies
455 targeting NBS1 co-depletes all detectable MRE11 but does not influence the levels of
456 TOPBP1 (Montales et al, 2022). This shows that the association of TOPBP1 with
457 NBS1 in egg extract is not as strong as the association of NBS1 with other members
458 of MRN, although it is possible that the antibodies used for depletion dislodge
459 TOPBP1 from NBS1.
460

461 What might be the function of the TOPBP1::NBS1 interaction(s)? In addition,
462 a related question is why did TOPBP1 evolve two disparate binding sites for NBS1,
463 positioned closely together at the amino terminus of the protein? We propose that
464 one function of the interaction is to recruit TOPBP1 to sites of damage so that it can
465 activate the ATR kinase. Three previous studies, all performed with frog egg
466 extracts, have implicated MRN in recruitment of TOPBP1 to stalled replication forks
467 (Lee and Dunphy, 2013), to an ATR-activating DNA structure comprised of M13
468 ssDNA to which primers are annealed (Duursma et al, 2013), and to 5kb linear
469 dsDNAs that mimic DSBs (Montales et al, 2022). Thus, it is clear that MRN is
470 important for how TOPBP1 arrives at sites of damage, and we propose that at least
471 one of the interactions defined in this paper plays a role in TOPBP1 recruitment for
472 the purpose of ATR signaling. But why does have TOPBP1 harbor more than one site
473 for interaction with NBS1? One possibility is that TOPBP1 also collaborates with
474 MRN is the physical repair of a DSB. Indeed, a recent study using Repair-seq to order
475 DNA repair proteins into common pathways showed that TOPBP1 clusters with
476 NBS1, MRE11, and RAD50 in that all four show a common repair defect upon their
477 depletion (Hussmann et al, 2021). Thus, it may be that TOPBP1 interacts with NBS1
478 differently for ATR signaling versus DNA repair, and if so, this would explain the
479 multiple binding sites. Clearly, further work, combining mutagenesis with functional
480 assays, is needed to clarify the roles of the two NBS1 binding sites on TOPBP1.
481
482 Another important question raised by our studies is how are the BRCT
483 domains from NBS1 and TOPBP1 interacting with one another? There is precedent

484 for BRCT domains to form both homo- and heterodimers. The best studied example
485 of this is found with the XRCC1 and LIG3 proteins (reviewed most recently by
486 London, 2020). XRCC1 has two BRCT domains, with BRCT2 being the one that binds
487 to itself as well as to the single BRCT domain within LIG3, which also interacts with
488 itself. Our previous work has shown that TOPBP1's BRCT1 and 2 domains can
489 interact with one another, and we have shown here that they also bind to NBS1
490 BRCT1. Thus, the TOPBP1::NBS1 system is similar to XRCC1::LIG3 in that both
491 systems can form homo- and heterotypic interactions. Recent structural analysis of
492 a human XRCC1 BRCT1::LIG3 BRCT dimer revealed that the two BRCT domains bind
493 one another largely through electrostatic interactions between residues located in
494 the alpha helix 1 portion of the respective domains (Hammel et al, 2021). Thus, it
495 will be of interest in future work to determine if a similar molecular interface
496 controls the interactions between TOPBP1 and NBS1.
497
498 Work presented here also reveals the remarkable versatility that TOPBP1's
499 BRCT0-2 region displays in its interactions with various binding partners. On the
500 one hand, there is the well-studied, phosphate-dependent interaction with RAD9Tail
501 (and other phospho-substrates), and on the other hand, as we have shown here, is a
502 very different mode of interaction, involving phosphate-free and direct binding to
503 NBS1. There are important differences between the phosphate-dependent and
504 phosphate-free modes of binding. For the former, a contiguous BRCT0-2 module is
505 required for efficient binding. In the case of the RAD9Tail, previous work has shown
506 that it is BRCT1 that contacts phosphate (Rappas et al, 2011), however BRCT1 alone

507 is not sufficient for the interaction (Figure 3B), and in data not shown we have
508 observed that BRCT0 also plays a positive role, as the BRCT0-2 region binds
509 RAD9Tail more efficiently than does the BRCT1&2 region. Thus, the BRCT0-2
510 continuum is needed for optimal binding in the phosphate -dependent mode, while
511 the phosphate-free mode can occur with isolated domains.
512
513 Another unexpected finding reported in this work is that interaction between
514 the TOPBP1 and NBS1 BRCT domains can occur in the context of truncated, and thus
515 improperly folded, domains. As shown in Figures 6B&C, for TOPBP1's BRCT1, we
516 used MBP fusions to ask if truncation of the intact domain would impede binding
517 and found that it did not. Indeed, we were able to show that a small peptide of just
518 29 amino acids can confer the ability to bind NBS1 when grafted on to MBP.
519 Similarly, we found that an even smaller peptide from TOPBP1's BRCT2 domain has
520 the same properties (Figures S2D&E). For NBS1, we found that removal of large
521 portions of BRCT1 did not impair binding to TOPBP1 (Figure 6E). In Figure 7A the
522 amino acid sequences of the three BRCT domains studied here are shown. For
523 TOPBP1, the residues that allow biding to NBS1, in a transferrable manner, are
524 highlighted in red. Also highlighted in red are the residues within NBS1 that
525 represent the minimal region sufficient for binding to TOPBP1, as defined by
526 deletion analysis (Figure 6E). We do not yet know if this sequence is transferrable,
527 but this seems likely. Also shown is the canonical arrangement of beta sheets and
528 alpha helices that promote proper folding of BRCT domains. While the minimally
529 defined region within BRCT2 shows good overlap with the corresponding sequence

530 from NBS1, there is very poor overlap between the two TOPBP1 sequences, perhaps
531 suggesting that TOPBP1's BRCT1 uses a different binding mode to interact with
532 NBS1 than does its BRCT2 domain.
533
534 Given these results with truncations we went on to ask if binding could still
535 occur when both partners where in a truncated form. We found that it could as
536 truncated TOPBP1 BRCT1 clearly interacts with a truncated form of NBS1 BRCT1
537 (Figure 6F). This interaction is specific as the NBS1 1-175 truncation binds both
538 intact TOPBP1 BRCT1 (91-179) and the truncated form (128-179), but further
539 truncation of NBS1 to yield 1-150 yields a protein unable to bind either intact or
540 truncated TOPBP1 BRCT1 (Figure 6F). Thus, truncated TOPBP1 BRCT1 binds to
541 NBS1 with the same specificity as the intact form. While these results are difficult to
542 reconcile with the notion that proper folding of an intact BRCT domain is a
543 prerequisite for its ability to specifically interact with any given binding partner,
544 they are not without precedent. Previous work has shown that a truncated form of
545 XRCC1 retains the ability to bind to LIG3 (Taylor et al, 1998). Indeed, this work
546 showed that a small peptide of 20 amino acids can be transferred to MBP, and this
547 confers binding to LIG3. Furthermore, binding of the peptide to LIG3 was
548 stoichiometric and of equivalent efficiency as the full-length XRCC1 protein (Taylor
549 et al, 1998). The sequence of XRCC1 BRCT2 is shown in Figure 7B, and the LIG3-
550 binding peptide underlined in black. Interestingly, this peptide maps to a similar
551 position within its BRCT domain as does the peptide from TOPBP1's BRCT1 that
552 confers binding to NBS1, as both sequences are comprised of the residues that form

553 beta sheet 3 within an intact domain, along with some flanking sequences (compare
554 Figures 7A and 7B). Curiously, however, recent structural studies of the
555 XRCC1::LIG3 complex have defined electrostatic interactions between residues
556 largely located in alpha helix 1 as comprising the binding interface for the
557 XRCC1::LIG3 interaction (Hammel et al, 2021). Thus, it is currently unclear how the
558 XRCC1 20mer peptide maintains key properties of the interaction with LIG3 when
559 the structural studies suggest the binding interface resides elsewhere in the domain.
560 This question is relevant to the work presented here, given that small peptides from
561 TOPBP1 can also confer binding to NBS1.
562
563 Lastly, we note that the crystal structure of human TOPBP1 in complex with a
564 phospho-peptide from RAD9 has been solved (Day et al, 2018), and thus it was of
565 interest to visualize where in this structure the two NBS1-binding peptides reside.
566 As shown in Figure 7C, left panel, much of the NBS1 binding peptide from TOPBP1's
567 BRCT1 is solvent-exposed and overlaps with the region that binds RAD9 (in Figure
568 7C the NBS1-binding peptide is colored in green and the RAD9 peptide is colored in
569 yellow). For the NBS1-binding peptide from BRCT2 we see that it is also solvent-
570 exposed and thus, in principle, able to interact with heterologous proteins (Figure
571 7C, right panel). Having defined these two regions of TOPBP1 as able to interact
572 with NBS1, the next important steps will be to first map the amino acids that are
573 crucial for the interaction and to then test these mutants in functional assays for
574 ATR activation and DNA repair, and such experiments are now in progress.
575

576 **Author contribution**

577 W.M.M. conceptualized the project, acquired the funding, and wrote the manuscript

578 together with O.H. O.H., K.R., and K.M. performed the experiments.

579

580 **Conflict of interest statement**

581 The authors declare no conflict of interest.

582

583 **Acknowledgments**

584 This work was supported by NIH grant R01GM12287. We thank Karlene Cimprich

585 for the gift of the GST-RAD9 Tail expression vector.

586 **References**
587
588 Bagge J, Oestergaard VH, Lisby M. Functions of TopBP1 in preserving genome
589 integrity during mitosis. Semin Cell Dev Biol. 2021 May;113:57-64. doi:
590 10.1016/j.semcdb.2020.08.009.
591
592 Beernink PT, Hwang M, Ramirez M, Murphy MB, Doyle SA, Thelen MP. Specificity of
593 protein interactions mediated by BRCT domains of the XRCC1 DNA repair protein. J
594 Biol Chem. 2005 Aug 26;280(34):30206-13. doi: 10.1074/jbc.M502155200.
595
596 Bigot N, Day M, Baldock RA, Watts FZ, Oliver AW, Pearl LH. Phosphorylation-
597 mediated interactions with TOPBP1 couple 53BP1 and 9-1-1 to control the G1 DNA
598 damage checkpoint. Elife. 2019 May 28;8:e44353. doi: 10.7554/eLife.44353.
599
600 Botuyan MV, Nominé Y, Yu X, Juranic N, Macura S, Chen J, Mer G. Structural basis of
601 BACH1 phosphopeptide recognition by BRCA1 tandem BRCT domains. Structure.
602 2004 Jul;12(7):1137-46. doi: 10.1016/j.str.2004.06.002. PMID: 15242590; PMCID:
603 PMC3652423.
604
605 Costa A, Diffley JFX. The Initiation of Eukaryotic DNA Replication. Annu Rev
606 Biochem. 2022 Jun 21;91:107-131. doi: 10.1146/annurev-biochem-072321-110228.
607
608 Cuneo MJ, Gabel SA, Krahn JM, Ricker MA, London RE. The structural basis for
609 partitioning of the XRCC1/DNA ligase III-α BRCT-mediated dimer complexes.
610 Nucleic Acids Res. 2011 Sep 1;39(17):7816-27. doi: 10.1093/nar/gkr419.
611
612 Day M, Rappas M, Ptasinska K, Boos D, Oliver AW, Pearl LH. BRCT domains of the
613 DNA damage checkpoint proteins TOPBP1/Rad4 display distinct specificities for
614 phosphopeptide ligands. Elife. 2018 Oct 8;7:e39979. doi: 10.7554/eLife.39979.
615
616 Day M, Oliver AW, Pearl LH. Phosphorylation-dependent assembly of DNA damage
617 response systems and the central roles of TOPBP1. DNA Repair (Amst). 2021
618 Dec;108:103232. doi: 10.1016/j.dnarep.2021.103232.
619
620 Dulic A, Bates PA, Zhang X, Martin SR, Freemont PS, Lindahl T, Barnes DE. BRCT
621 domain interactions in the heterodimeric DNA repair protein XRCC1-DNA ligase III.
622 Biochemistry. 2001 May 22;40(20):5906-13. doi: 10.1021/bi002701e.
623
624 Duursma AM, Driscoll R, Elias JE, Cimprich KA. A role for the MRN complex in ATR
625 activation via TOPBP1 recruitment. Mol Cell. 2013 Apr 11;50(1):116-22. doi:
626 10.1016/j.molcel.2013.03.006.
627
628 Gerloff DL, Woods NT, Farago AA, Monteiro AN. BRCT domains: A little more than
629 kin, and less than kind. FEBS Lett. 2012 Aug 14;586(17):2711-6. doi:
630 10.1016/j.febslet.2012.05.005.
631

632 Hammel M, Rashid I, Sverzhinsky A, Pourfarjam Y, Tsai MS, Ellenberger T, Pascal JM,
633 Kim IK, Tainer JA, Tomkinson AE. An atypical BRCT-BRCT interaction with the
634 XRCC1 scaffold protein compacts human DNA Ligase IIIα within a flexible DNA
635 repair complex. Nucleic Acids Res. 2021 Jan 11;49(1):306-321. doi:
636 10.1093/nar/gkaa1188.
637
638 Hou WH, Chen SH, Yu X. Poly-ADP ribosylation in DNA damage response and cancer
639 therapy. Mutat Res Rev Mutat Res. 2019 Apr-Jun;780:82-91. doi:
640 10.1016/j.mrrev.2017.09.004.
641
642 Hussmann JA, Ling J, Ravisankar P, Yan J, Cirincione A, Xu A, Simpson D, Yang D,
643 Bothmer A, Cotta-Ramusino C, Weissman JS, Adamson B. Mapping the genetic
644 landscape of DNA double-strand break repair. Cell. 2021 Oct 28;184(22):5653-
645 5669.e25. doi: 10.1016/j.cell.2021.10.002.
646
647 Kim A, Montales K, Ruis K, Senebandith H, Gasparyan H, Cowan Q, Michael WM.
648 Biochemical analysis of TOPBP1 oligomerization. DNA Repair (Amst). 2020
649 Dec;96:102973. doi: 10.1016/j.dnarep.2020.102973.
650
651 Lee J, Dunphy WG. The Mre11-Rad50-Nbs1 (MRN) complex has a specific role in the
652 activation of Chk1 in response to stalled replication forks. Mol Biol Cell. 2013
653 May;24(9):1343-53. doi: 10.1091/mbc.E13-01-0025.
654
655 Leung CC, Glover JN. BRCT domains: easy as one, two, three. Cell Cycle. 2011 Aug
656 1;10(15):2461-70. doi: 10.4161/cc.10.15.16312.
657
658 London RE. The structural basis of XRCC1-mediated DNA repair. DNA Repair
659 (Amst). 2015 Jun;30:90-103. doi: 10.1016/j.dnarep.2015.02.005.
660
661 London RE. XRCC1 - Strategies for coordinating and assembling a versatile DNA
662 damage response. DNA Repair (Amst). 2020 Sep;93:102917. doi:
663 10.1016/j.dnarep.2020.102917.
664
665 Ma M, Rodriguez A, Sugimoto K. Activation of ATR-related protein kinase upon DNA
666 damage recognition. Curr Genet. 2020 Apr;66(2):327-333. doi: 10.1007/s00294-
667 019-01039-w.
668
669 McCarthy-Leo C, Darwiche F, Tainsky MA. DNA Repair Mechanisms, Protein
670 Interactions and Therapeutic Targeting of the MRN Complex. Cancers (Basel). 2022
671 Oct 27;14(21):5278. doi: 10.3390/cancers14215278.
672
673 Montales K, Kim A, Ruis K, Michael WM. Structure-function analysis of TOPBP1's
674 role in ATR signaling using the DSB-mediated ATR activation in Xenopus egg
675 extracts (DMAX) system. Sci Rep. 2021 Jan 11;11(1):467. doi: 10.1038/s41598-020-
676 80626-1.
677

678 Montales K, Ruis K, Lindsay H, Michael WM. MRN-dependent and independent
679 pathways for recruitment of TOPBP1 to DNA double-strand breaks. PLoS One. 2022
680 Aug 2;17(8):e0271905. doi: 10.1371/journal.pone.0271905.
681
682 Morishima K, Sakamoto S, Kobayashi J, Izumi H, Suda T, Matsumoto Y, Tauchi H, Ide
683 H, Komatsu K, Matsuura S. TopBP1 associates with NBS1 and is involved in
684 homologous recombination repair. Biochem Biophys Res Commun. 2007 Nov
685 3;362(4):872-9. doi: 10.1016/j.bbrc.2007.08.086.
686
687 Moudry P, Watanabe K, Wolanin KM, Bartkova J, Wassing IE, Watanabe S, Strauss R,
688 Troelsgaard Pedersen R, Oestergaard VH, Lisby M, Andújar-Sánchez M, Maya-
689 Mendoza A, Esashi F, Lukas J, Bartek J. TOPBP1 regulates RAD51 phosphorylation
690 and chromatin loading and determines PARP inhibitor sensitivity. J Cell Biol. 2016
691 Feb 1;212(3):281-8. doi: 10.1083/jcb.201507042.
692
693 Paull TT. Mechanisms of ATM Activation. Annu Rev Biochem. 2015;84:711-38. doi:
694 10.1146/annurev-biochem-060614-034335.
695
696 Rappas M, Oliver AW, Pearl LH. Structure and function of the Rad9-binding region of
697 the DNA-damage checkpoint adaptor TopBP1. Nucleic Acids Res. 2011
698 Jan;39(1):313-24. doi: 10.1093/nar/gkq743.
699
700 Reginato G, Cejka P. The MRE11 complex: A versatile toolkit for the repair of broken
701 DNA. DNA Repair (Amst). 2020 Jul-Aug;91-92:102869. doi:
702 10.1016/j.dnarep.2020.102869.
703
704 Reinhardt HC, Yaffe MB. Phospho-Ser/Thr-binding domains: navigating the cell
705 cycle and DNA damage response. Nat Rev Mol Cell Biol. 2013 Sep;14(9):563-80. doi:
706 10.1038/nrm3640.
707
708 Ruis K, Huynh O, Montales K, Barr NA, Michael WM. Delineation of a minimal
709 topoisomerase II binding protein 1 for regulated activation of ATR at DNA double-
710 strand breaks. J Biol Chem. 2022 Jul;298(7):101992. doi:10.1016/j.jbc.2022.101992.
711
712 Sheng ZZ, Zhao YQ, Huang JF. Functional Evolution of BRCT Domains from Binding
713 DNA to Protein. Evol Bioinform Online. 2011;7:87-97. doi: 10.4137/EBO.S7084.
714
715 Shiotani B, Nguyen HD, Håkansson P, Maréchal A, Tse A, Tahara H, Zou L. Two
716 distinct modes of ATR activation orchestrated by Rad17 and Nbs1. Cell Rep. 2013
717 May 30;3(5):1651-62. doi: 10.1016/j.celrep.2013.04.018.
718
719 Syed A, Tainer JA. The MRE11-RAD50-NBS1 Complex Conducts the Orchestration of
720 Damage Signaling and Outcomes to Stress in DNA Replication and Repair. Annu Rev
721 Biochem. 2018 Jun 20;87:263-294. doi: 10.1146/annurev-biochem-062917-012415.
722

723 Taylor RM, Wickstead B, Cronin S, Caldecott KW. Role of a BRCT domain in the
724 interaction of DNA ligase III-alpha with the DNA repair protein XRCC1. Curr Biol.
725 1998 Jul 16;8(15):877-80. doi: 10.1016/s0960-9822(07)00350-8.
726
727 Van Hatten RA, Tutter AV, Holway AH, Khederian AM, Walter JC, Michael WM. The
728 Xenopus Xmus101 protein is required for the recruitment of Cdc45 to origins of
729 DNA replication. J Cell Biol. 2002 Nov 25;159(4):541-7. doi:
730 10.1083/jcb.200207090.
731
732 Wan B, Hang LE, Zhao X. Multi-BRCT scaffolds use distinct strategies to support
733 genome maintenance. Cell Cycle. 2016 Oct;15(19):2561-2570. doi:
734 10.1080/15384101.2016.1218102.
735
736 Wan B, Wu J, Meng X, Lei M, Zhao X. Molecular Basis for Control of Diverse Genome
737 Stability Factors by the Multi-BRCT Scaffold Rtt107. Mol Cell. 2019 Jul 25;75(2):238-
738 251.e5. doi: 10.1016/j.molcel.2019.05.035.
739
740 Wardlaw CP, Carr AM, Oliver AW. TopBP1: A BRCT-scaffold protein functioning in
741 multiple cellular pathways. DNA Repair (Amst). 2014 Oct;22:165-74. doi:
742 10.1016/j.dnarep.2014.06.004.
743
744 Yan S, Lindsay HD, Michael WM. Direct requirement for Xmus101 in ATR-mediated
745 phosphorylation of Claspin bound Chk1 during checkpoint signaling. J Cell Biol.
746 2006 Apr 24;173(2):181-6. doi: 10.1083/jcb.200601076.
747
748 Yoo HY, Kumagai A, Shevchenko A, Shevchenko A, Dunphy WG. The Mre11-Rad50-
749 Nbs1 complex mediates activation of TopBP1 by ATM. Mol Biol Cell. 2009
750 May;20(9):2351-60. doi: 10.1091/mbc.e08-12-1190.

751 **Main Figures and Legends**

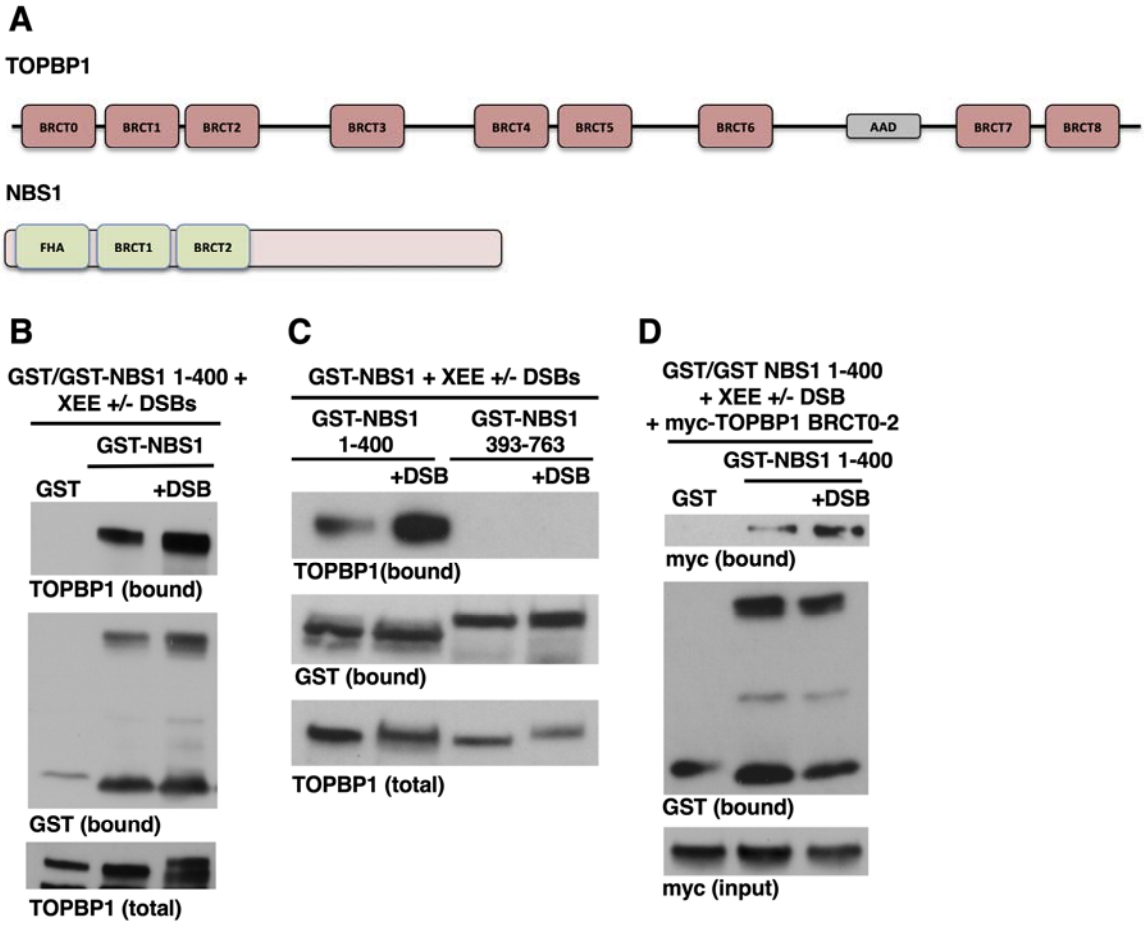

752

753 **Figure 1. NBS1 and TOPBP1 interact in frog egg extracts.**

754 **A.** Schematic representation of the proteins of interest. TOPBP1 contains 9 BRCT
755 domains while NBS1 contains two BRCT domains, as well as an N-terminal FHA
756 domain. **B.** A GST pull-down assay was performed, as described in the Methods, with
757 the indicated GST proteins. This was done in the presence of egg extract, with
758 optionally added DSBs, and the presence of endogenous TOPBP1 in the bound
759 fraction was detected by Western blot. The experiment shown is representative of
760 two independently performed biological replicates. **C.** Same as (B) except GST-NBS1
761 393-763 was included. The experiment shown is representative of two

762 independently performed biological replicates. **D.** Myc-tagged TOPBP1 BRCT0-2,
763 produced by IVTT, was added to XEE, and DSBs were optionally included, as
764 indicated. The indicated GST proteins were also included, and then the samples
765 were then processed as in (B). The experiment shown is representative of two
766 independently performed biological replicates.
767
768

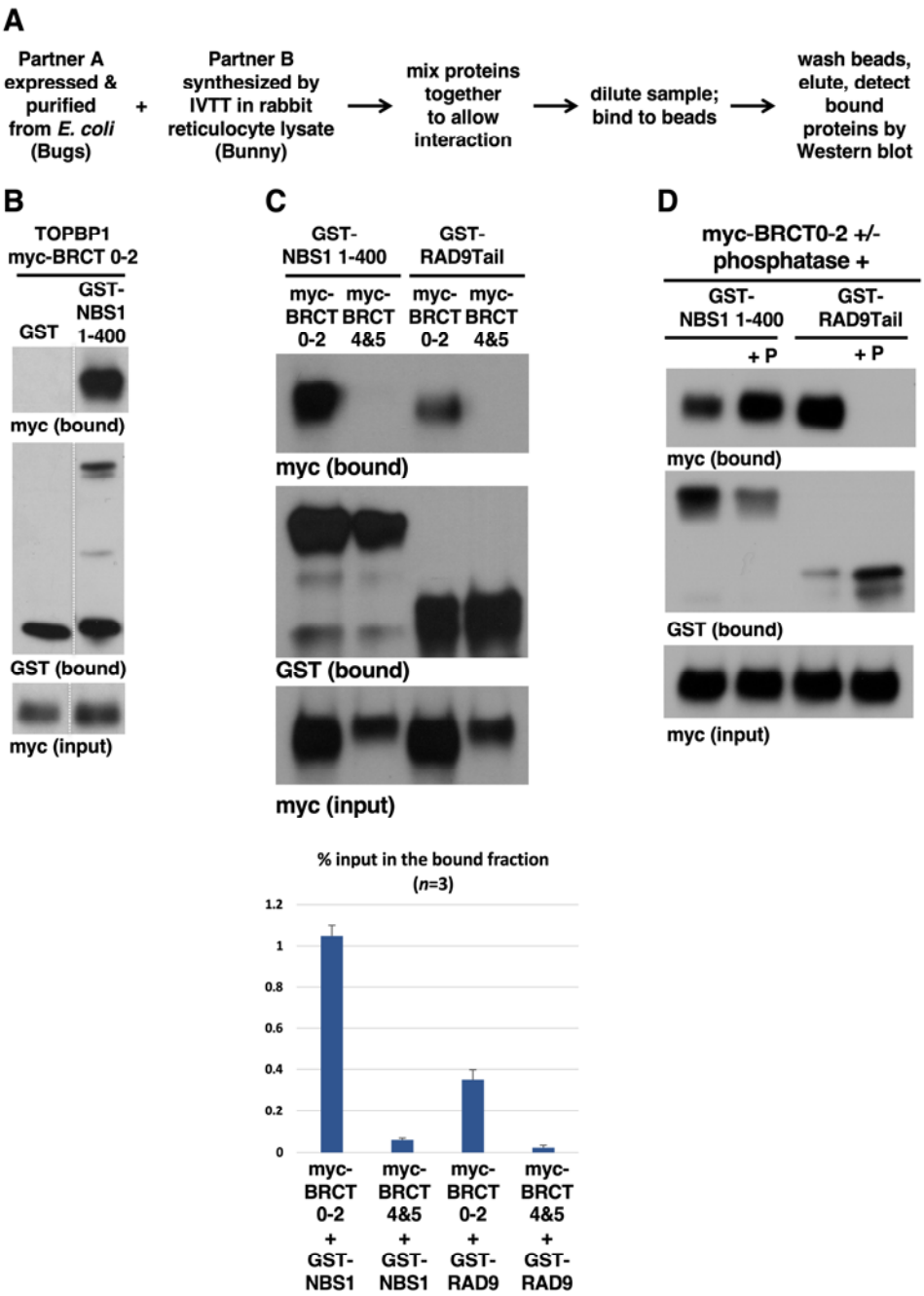

769

770 **Figure 2. The Bugs-Bunny system recapitulates a phosphate-independent**

771 **interaction between NBS1 and TOPBP1.**

772 **A.** Overview of the Bugs-Bunny protein binding assay system. **B.** The indicated GST

773 proteins, expressed and purified from *E. coli*, were incubated in IVTT reactions

774 expressing myc-tagged TOPBP1 BRCT0-2. The samples were then processed for the

775 GST pull-down assay as described in the Methods. Samples of the total binding
776 reaction, taken prior to dilution, were also probed for myc, showing that the myc-
777 tagged proteins were present in equivalent amounts across all the samples (lane
778 "input"). The experiment shown is representative of two independently performed
779 biological replicates. We note that the image shown is derived from a larger gel, and
780 the irrelevant samples were removed. The white dashed line depicts where the gel
781 was spliced together. The full gel with all original samples is shown in Figure S1A.
782 **C.** A GST pull-down assay was performed, as in part A, with the indicated GST- and
783 myc-tagged proteins. The experiment shown is representative of three
784 independently performed biological replicates. Quantification of all three
785 experiments is shown in the graph. Please see Methods for how these experiments
786 were quantified. **D.** A GST pull-down assay was performed, as in part A, with the
787 indicated GST proteins and myc-tagged TOPBP1 BRCT0-2. In this experiment
788 lambda phosphatase was optionally added, as indicated. The experiment shown is
789 representative of two independently performed biological replicates.
790
791

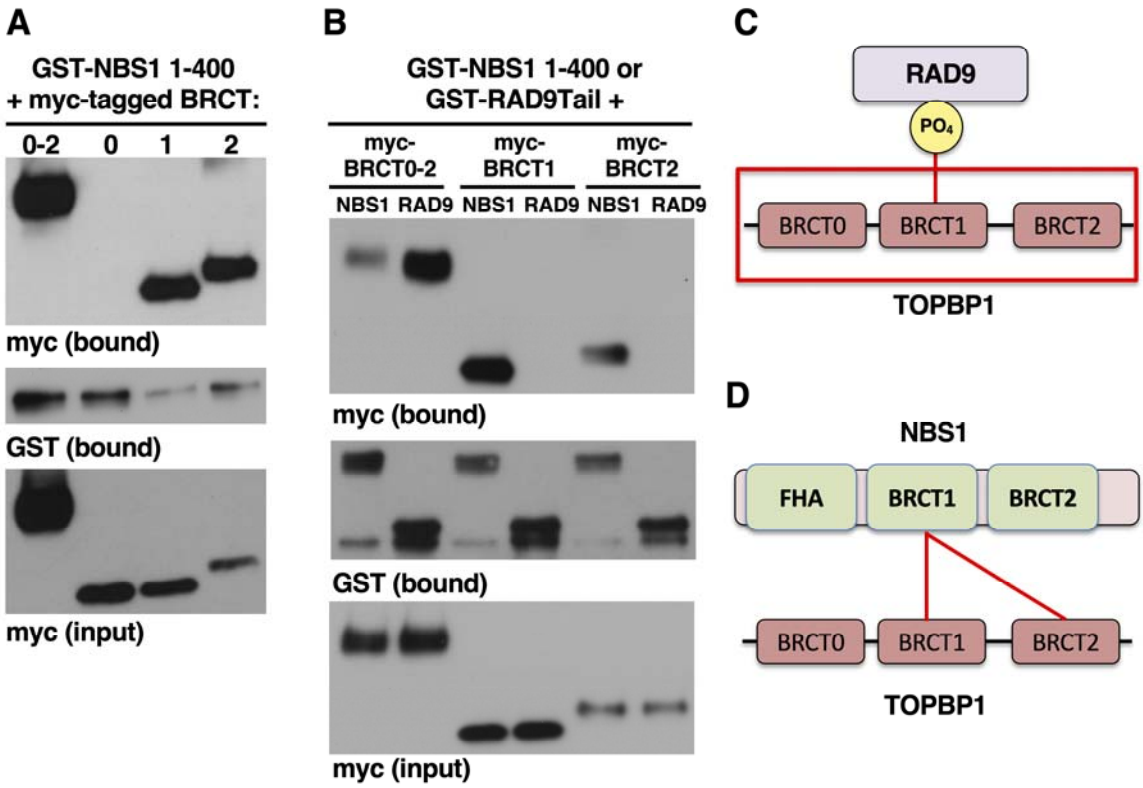

Figure 3. NBS1 independently binds to both BRCT1 and BRCT2 from TOPBP1. **A.** GST pull-down assays, using GST-NBS1 1-400 with myc-tagged versions of TOPBP1's N-terminal BRCT domains, were performed exactly as in Figure 2B. **B.** GST pull-down assays, using GST-NBS1 1-400 or GST-RAD9Tail together with myc-tagged versions of TOPBP1's N-terminal BRCT domains, were performed exactly as in Figure 2B. The experiments shown are representative of two independently performed biological replicates. **C-D.** Cartoons highlighting the different ways that RAD9Tail and NBS1 interact with TOPBP1's BRCT0-2 region. See text for details.

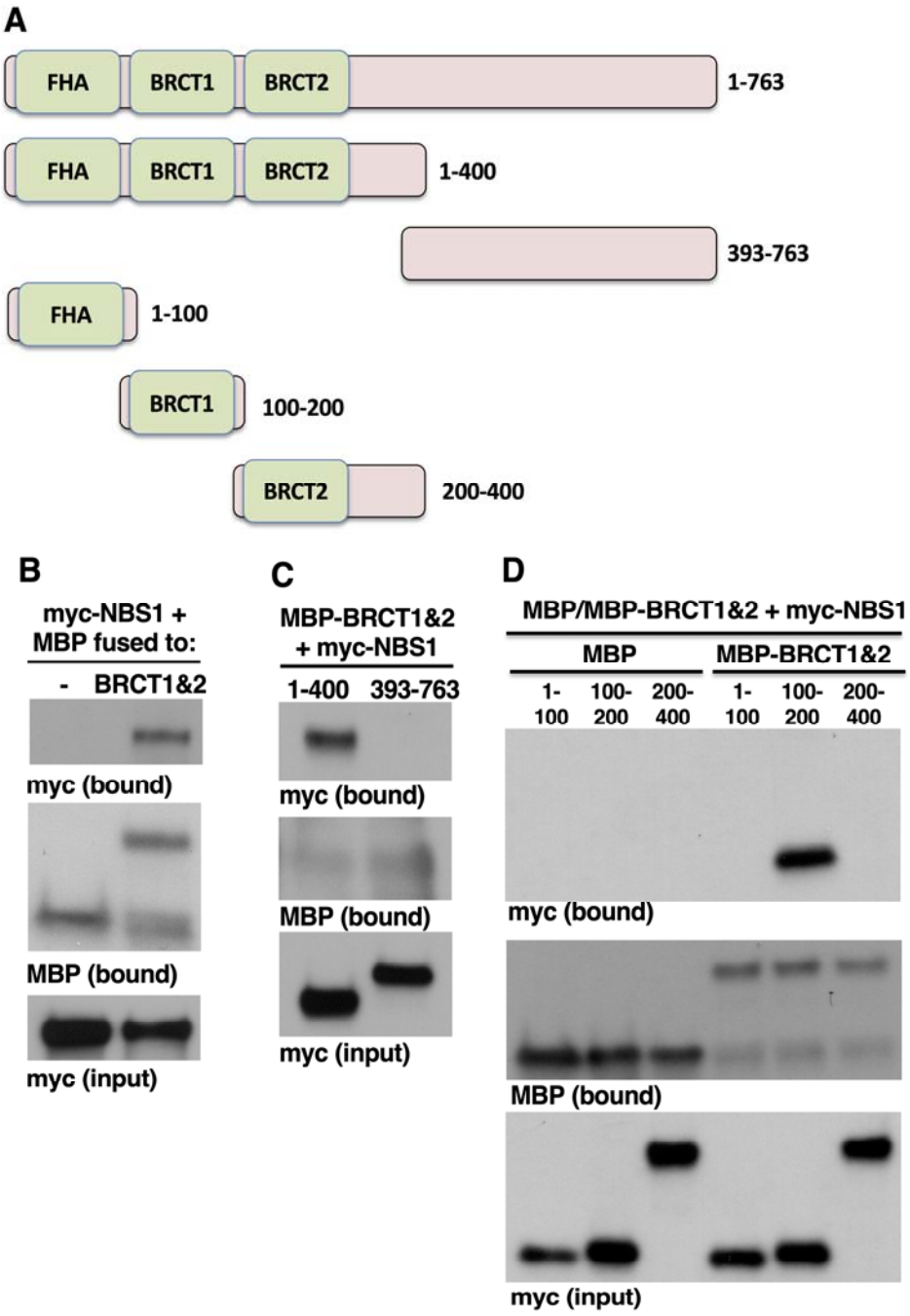

Figure 4. NBS1 uses its BRCT1 to bind TOPBP1.

A. Cartoons summarizing the domains located within the N-terminus of NBS1 and the various truncations used in the binding assays. **B.** MBP pull-down assays were performed using either MBP alone or MBP fused to TOPBP1's BRCT1&2 domains, together with myc-tagged and full-length NBS1. The experiment shown is

809 representative of two independently performed biological replicates. **C.** MBP pull-
810 down assays were performed using MBP-TOPBP1 BRCT1&2, together with the
811 indicated myc-tagged forms of NBS1. The experiment shown is representative of
812 two independently performed biological replicates. **D.** MBP pull-down assays were
813 performed using either MBP alone or MBP fused to TOPBP1's BRCT1&2 domains,
814 together with the indicated myc-tagged forms of NBS1. The experiment shown is
815 representative of two independently performed biological replicates.
816
817

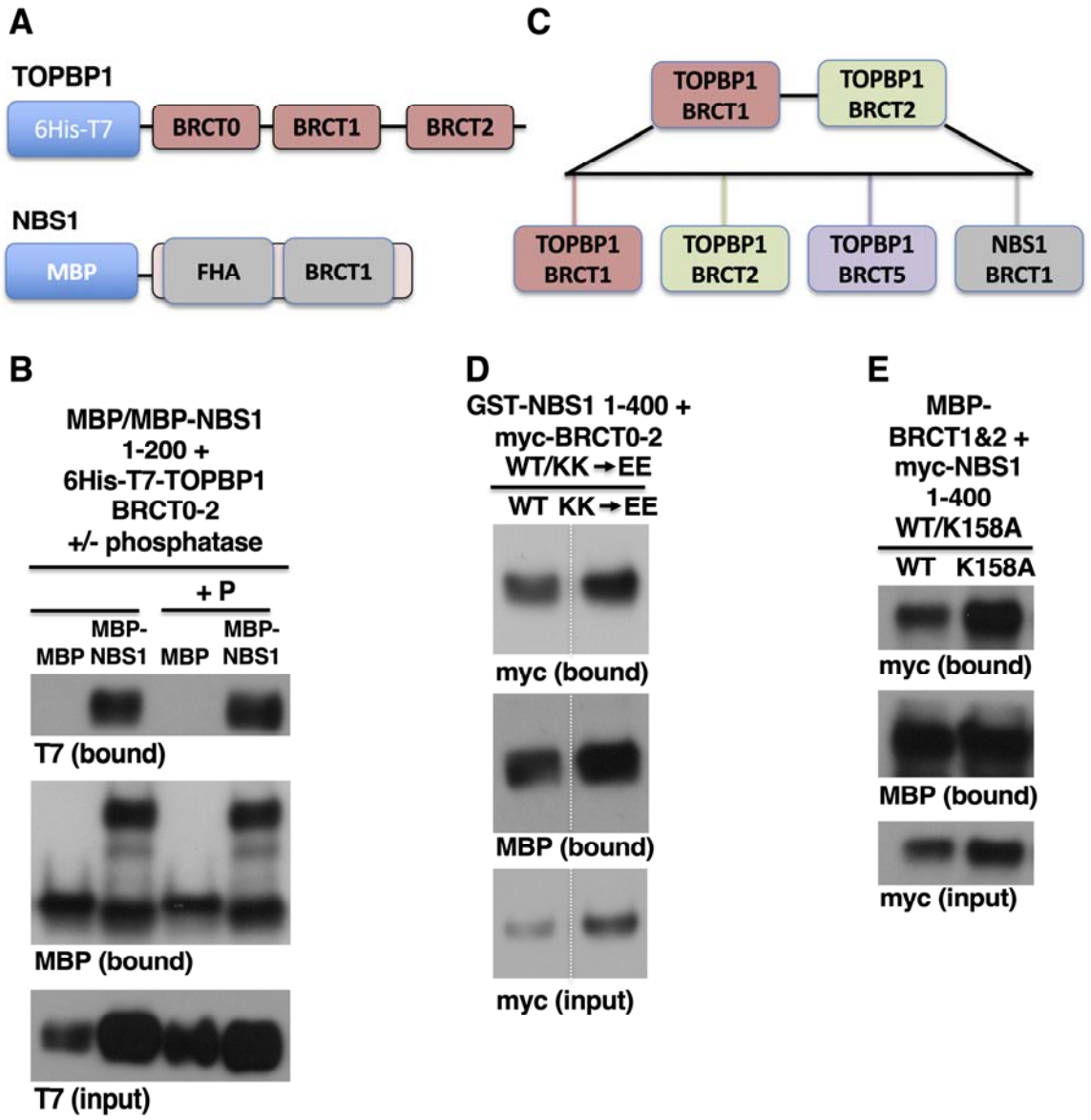

Figure 5. Direct interaction between TOPBP1 and NBS1 and the role of PBPs in the interaction.

A. Cartoons showing the recombinant proteins used in the binding assay displayed in part B. **B.** All the proteins used in this binding assay were expressed and purified from *E. coli*. Shown is an MBP pull-down assay with either MBP alone or MBP fused to NBS1 1-200, together with 6His-T7 tagged TOPBP1 BRCT0-2. The binding reaction was performed in the presence of a 1% BSA solution, to suppress non-

826 specific binding to the maltose resin. As in Figure 2D, phosphatase was optionally
827 included (as indicated by the "P"). The experiment shown is representative of two
828 independently performed biological replicates. **C.** A schematic summarizing the
829 disparate BRCT domains that are known to bind the TOPBP1 BRCT1&2 region. All of
830 these domains contain a PBP. **D.** GST pull-down assays, using GST-NBS1 1-400 with
831 myc-tagged TOPBP1 BRCT0-2, were performed exactly as in Figure 2B. Shown are
832 both the wild type (WT) and K155K249 to EE ("KK->EE") forms of TOPBP1 BRCT0-
833 2. The experiment shown is representative of two independently performed
834 biological replicates. We note that the image shown is derived from a larger gel, and
835 the irrelevant samples were removed. The white dashed line depicts where the gel
836 was spliced together. The full gel with all original samples is shown in Figure S1B.
837 **E.** An MBP pull-down assay was performed with MBP-TOPBP1 BRCT1&2 together
838 with either wild type ("WT") or the lysine 158 to alanine ("K158A") forms of myc-
839 tagged NBS1. 1-400. The experiment shown is representative of two independently
840 performed biological replicates.
841
842

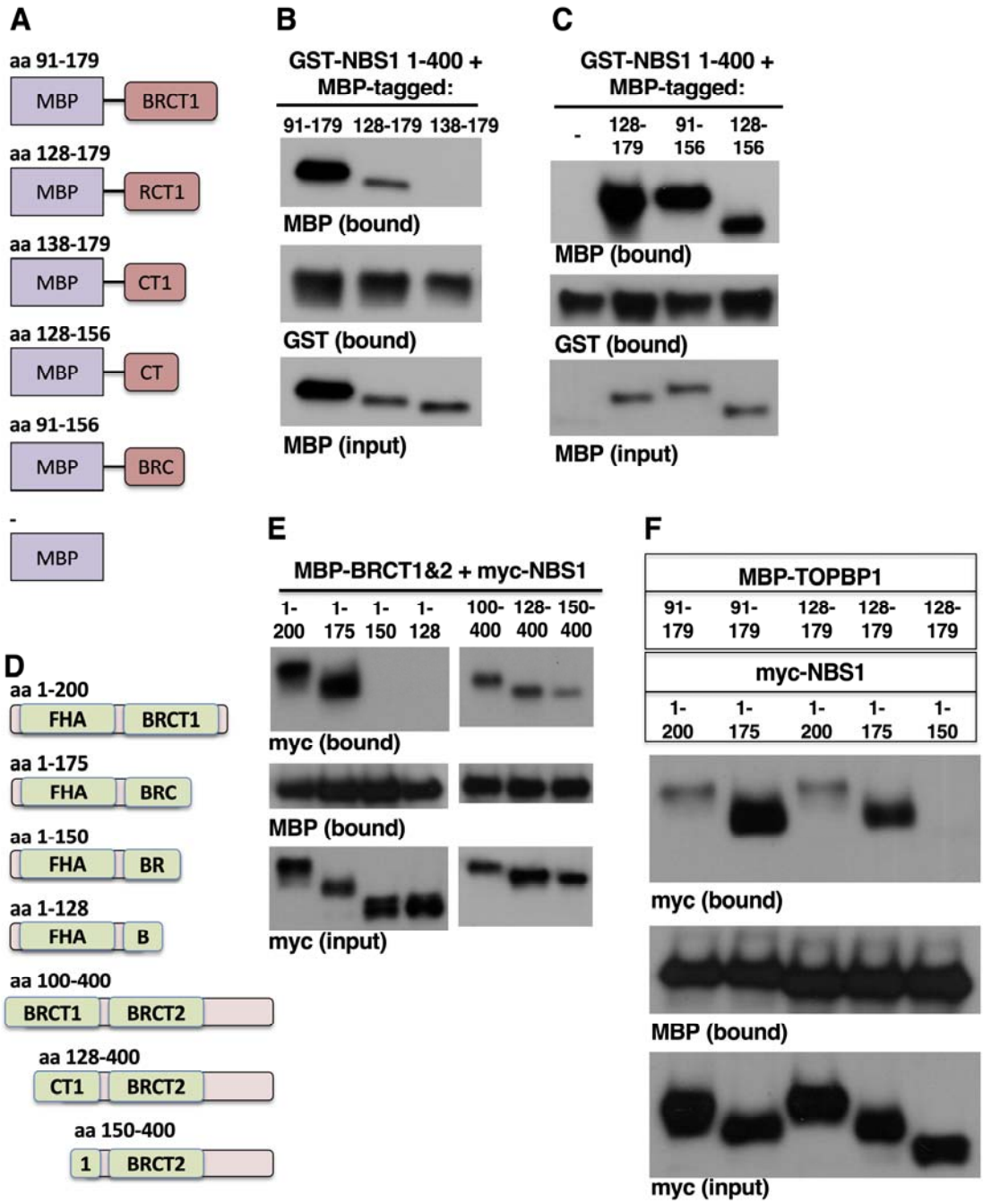

843

844 **Figure 6. Intact BRCT domains are dispensable for the TOPBP1::NBS1**

845 **interaction.**

846 **A.** Cartoons summarizing the various TOPBP1 BRCT1 truncations used in the

847 binding assays. These MBP-fusion proteins were produced by IVTT and used in pull-

848 down assays with recombinant GST-NBS1 1-400. **B-C.** GST pull-down assays, using

849 GST-NBS1 1-400 together with the indicated MBP-tagged TOPBP1 derivatives. The
850 experiments shown are representative of two independently performed biological
851 replicates. **D.** Cartoons summarizing the various NBS1 truncations used in the
852 binding assays. **E.** MBP pull-down assays using MBP-TOPBP1 BRCT1&2 together
853 with the indicated myc-tagged NBS1 derivatives. The experiment shown is
854 representative of two independently performed biological replicates. **F.** MBP pull-
855 down assays were performed with the indicated proteins. In this experiment, both
856 the MBP-TOPBP1 derivatives and the myc-NBS1 derivatives were produced by
857 IVTT. The experiment shown is representative of two independently performed
858 biological replicates.

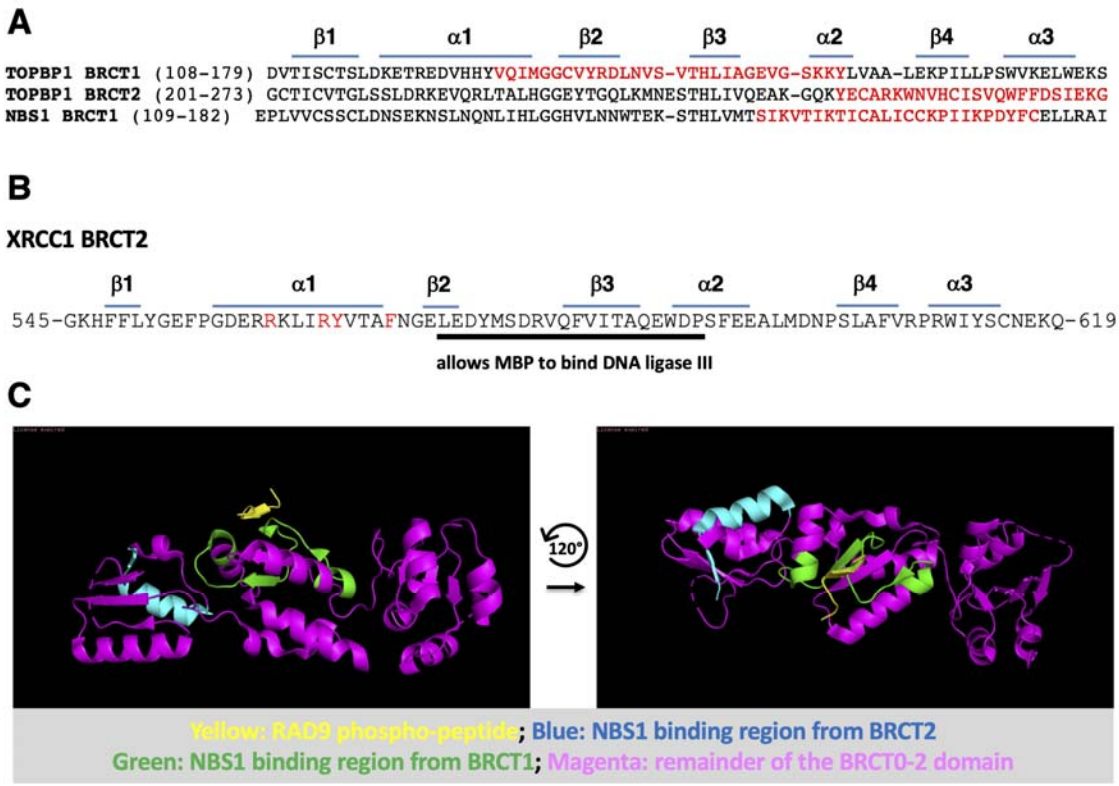

Figure 7. Summary of the BRCT domain delineation analyses.

A. The amino acid sequences of the indicated domains are displayed. Above the sequences are the positions of either beta sheets or alpha helices, as indicated. Highlighted in red for TOPBP1 are the small stretches of amino acids that confer binding to NBS1 when fused to MBP. Highlighted in red for NBS1 is the region of BRCT1 that binds TOPBP1, as defined by deletion analysis. **B.** The human XRCC1 BRCT2 sequence is shown. Underlined in black is the small region that confers binding to LIG3 when fused to MBP, as shown in Taylor et al, 1998, and highlighted in red are residues shown by Hammel et al, 2021 to be required for binding to LIG3. **C.** Two views of the crystal structure of the human TOPBP1 BRCT0-2 region in complex with a RAD9 phospho-peptide. The images were generated using Pymol structure view software and data set PDB ID: 6HM5.